

MARKOV RANDOM FIELD MODEL AND FUZZY FORMALISM-BASED DATA MODELING FOR THE SEA-FLOOR CLASSIFICATION

M.Mignotte ⁺ *C.Collet* ⁺ *P.Pérez* ^{*} *P.Bouthemy* ^{*}

⁺ Laboratoire GTS (Groupe de Traitement du Signal)
Ecole Navale, Lanvéoc-Poulmic, BP 600 - 29240 Brest-Naval France.

e-mail: collet@ecole-navale.fr

^{*} IRISA/INRIA, Campus Universitaire de Beaulieu, 35042 Rennes cedex, France.

e-mail: name@irisa.fr

ABSTRACT

In this paper we propose an original and statistical method for the sea-floor segmentation and its classification into five kinds of regions: sand, pebbles, rocks, ridges and dunes. The proposed method is based on the identification of the cast shadow shapes for each sea-bottom type and consists in four stages of processing. Firstly, the input image is segmented into two kinds of regions: shadow (corresponding to a lack of acoustic reverberation behind each object lying on the sea-bed) and sea-bottom reverberation. Secondly, the image of the contours of the detected cast shadows is partitioned into sub-windows from which a relevant geometrical feature vector is extracted. A pre-classification by a fuzzy classifier is thus required to initialize the third stage of processing. Finally, a Markov Random Field (MRF) model is employed to specify homogeneity properties of the desired segmentation map. A Bayesian estimate of this map is computed using a deterministic relaxation algorithm. Reported experiments demonstrate that the proposed approach yields promising results to the problem of sea-floor classification.

keywords: *sonar imagery, sea-bed classification, Markov Random Field (MRF), fuzzy logic.*

1. INTRODUCTION

High-resolution sidescan sonar plays an important role in underwater sensing due to its capability of providing high-quality acoustic imaging of the sea-bed. One of its application is the automatic segmentation and classification of the sea-bottom. Segmentation of sea-floor aims at partitioning the acoustic image into homogeneous regions with respect to certain geological characteristics. The goal of the classification task is then to assign these different geoacoustic regions to sea-floor classes such as, “sand”, “pebbles”, etc. These tasks can be essential in a wide range of applications such as geological survey (cartography, geophysical exploration, etc.), ocean engineering (pipeline and cable surveying, etc.), military field, or to improve the detection and classification of manufactured objects lying on sea-floors [1]. Basically, a general procedure for sea-floor classification consists in doing: 1) data acquisition (followed by a possible preprocessing); 2) feature extraction over small two dimensional areas within the image (aiming at reducing the informations contained in sub-image to a relevant feature vector); 3) selection of a classification algorithm and finally; 4) classification of each sub-image.

▷ For the feature extraction step, a commonly used approach consists in considering the sea-floor sonar images as highly textured. Under this assumption, we can use either the input image, i.e., the grey-levels themselves [2], or some relevant textural feature measures on it, such as the grey level co-occurrence matrices [3],[4],[5], the autoregressive parameters [6],[7], spectral or fractal measures [5],[8],[9]. Nevertheless, in many cases, the input sonar image is strongly corrupted by speckle noise [10] and depending the noise and sonar characteristics that affect signal strength [11], images can be apparently different for the same

¹ **Acknowledgments:** The authors thank **GESMA** (Groupe d'Étude Sous Marine de l'Atlantique, Brest, France) for having provided numerous real sonar pictures, and **DGA**, (Direction Générale de l'Armement, French Ministry of Defense) for partial financial support of this work (student grant).

sea-floor. For this reason, the extracted textural features, computed directly on the grey level, may be not very representative of the terrain morphology. Instead of using directly these grey levels, or some textural features on it, an alternative approach consists in using the output of an unsupervised two-class Markovian segmentation of the sonar image [12] and a pattern recognition methodology. The basic idea is to identify the detected cast shadow shapes of the different morphological elements (such as ridges, pebbles, etc.) located on the sea-floor.

▷ For the classification step, different kinds of methods can be applied. A first approach corresponds to statistical discrimination such as Maximum Likelihood classifier [6] or Maximum A Posteriori (MAP) classifier. An inherent drawback of these approaches, however, is that it is usually assumed that the underlying probability distribution function of each class is known as well as computable. Unlike statistical methods, neural networks [2],[4],[5],[7],[8],[13],[14], make no *a priori* assumptions about the distribution of their inputs. On the other hand, they usually require a learning step training data which can be problematic. In order to model *a priori* partially defined information as well as exact knowledge about the cast shadow shape corresponding to each sea-bottom type, an alternative approach, that we will adopt in this paper, consists in exploiting these *a priori* information within a fuzzy classification scheme. This fuzzy formalism allows also to take into account the mixture of classes of different nature within a sub-image that can occurs in sea-floor classification context. In order to obtain an accurate segmentation map, contextual information (i.e., relations between feature measures computed on adjacent sub-images) can be taken into account. To this end, we can efficiently use MRF modeling which is appropriate to specify spatial dependency between adjacent sub-images by means of *a priori* label field distribution [15].

In this paper, we propose a cast shadow shape fuzzy recognition approach combined with a Markovian segmentation model to solve the sea-bed segmentation-and-classification problem. The proposed method is divided into four steps: 1) unsupervised two-class segmentation; 2) feature extraction; 3) fuzzy pre-classification; 4) Markovian segmentation. The block diagram of the implemented system is shown in Fig. 1. In Section 2, we describe the feature extraction step. Section 3 presents the fuzzy classification step, whereas Section 4 introduces the MRF model for the segmentation step. Results and conclusion are given respectively in Section 5 and 6.

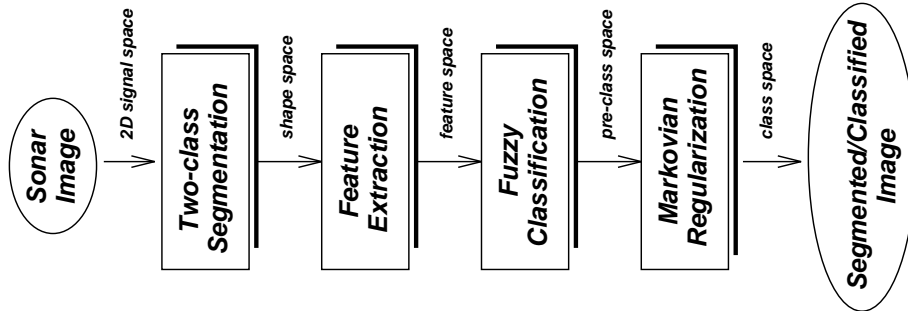


Figure 1: Overview of the proposed sea-bed classification scheme.

2. FEATURE EXTRACTION STEP

The feature extraction step, we consider, does not directly handle the grey level of the image but exploits the result of an unsupervised two-class (*shadow* and *reverberation* areas) Markovian segmentation of the input sonar image as explained in [12]. This segmentation is then high-pass filtered and binarized in order to extract the contour of each detected cast shadow. Then, the resulting edge image is partitioned in small two-dimensional sub-windows from which feature vector are extracted. The aim of this feature extraction process is to simplify the representation of the shadow shapes created by the different sea-floor types, and to cope with a relevant parameter vector giving maximal information about the extracted shadow

profiles. Thus, each vector is associated to a sub-image. In order to distinguish between the cast shadow shapes of ridges, dunes (whose cast shadow shapes are geometrically elongated and parallel), pebbles, stones (corresponding to elements with random orientation), we have selected geometrical features. For every cast shadow outline contained in the considered sub-window, we compute the following measures:

- **The compactness:** which evaluates the degree of compactness of the shape and is defined by:

$$C = \frac{4\pi S}{l^2}$$

where l and S stands respectively for the perimeter and the surface area delimited by the outline.

- **The elongation:** we compute for the cast shadow principal axis elongation ξ (defined as the standard deviation along the principal axis divided by the standard deviation along the smallest axis). This parameter is given by the eigenvalues correlation matrix \mathcal{C} and is computed from coordinates of points in the cast shadow outline:

$$\xi = \sqrt{\frac{(c_{xx} + c_{yy} + \sqrt{(c_{xx} - c_{yy})^2 + 4c_{xy}^2})}{(c_{xx} + c_{yy} - \sqrt{(c_{xx} - c_{yy})^2 + 4c_{xy}^2})}}$$

with:

$$c_{xx} = \frac{1}{N_\Gamma} \sum_{s \in \Gamma} (x_s - x_G)^2$$

$$c_{yy} = \frac{1}{N_\Gamma} \sum_{s \in \Gamma} (y_s - y_G)^2$$

$$c_{xy} = \frac{1}{N_\Gamma} \sum_{s \in \Gamma} (x_s - x_G)(y_s - y_G)$$

where the summation is over all the N_Γ pixels s of coordinates (x, y) on the outline Γ . (x_G, y_G) is the center of gravity of Γ .

- **The orientation:** we compute the orientation of the shadow principal axis defined by:

$$\alpha = \arctan\left(\frac{-c_{xx} + c_{yy} + \sqrt{(c_{xx} - c_{yy})^2 + 4c_{xy}^2}}{2c_{xy}}\right)$$

Finally, a set of four features (invariant to rotation) can be derived from these geometrical parameters computed on each outline. For each sub-window, we compute: 1.) “The mean compactness” (C_{moy}) of the set of outlines contained in the sub-window to be classified; 2.) “The directivity” that allows to know if the detected cast shadows within the considered sub-window have a common orientation. To this end, we compute the variance of orientation parameter: σ_α^2 ; 3.) “The maximal elongation cast shadow” (ξ_{max}) contained within the considered sub-window; and finally; 4. “The maximal size cast shadow outline” (N_{max}). Once these four parameters have been computed for each sub-window, they make up the feature vector that will be used for the fuzzy pre-classification step.

3. FUZZY CLASSIFICATION

In order to take into account these heterogeneous features, a classification module based on fuzzy pattern recognition is defined. This formalism is well suited to model our *a priori* knowledge about the cast shadow shapes for each sea-bottom type. It can also efficiently takes into account the mixture of classes of different natures that can occurs within a sub-image to be classified.

If there are no contours in the considered sub-window, we can assign it to the “sand” class. We have now to distinguish between four classes: “ridges”, “dunes”, “pebbles”, “rocks”. Let us define the notation. Each feature vector x_k computed on sub-window k is described by the four geometrical features $x_k = (F_{k1} = C_{moy}, F_{k2} = \sigma_\alpha^2, F_{k3} = \xi_{max}, F_{k4} = N_{max})$, and can be assigned to five distinct classes w_i

($w_0 = \text{sand}$, $w_1 = \text{ridges}$, $w_2 = \text{dunes}$, $w_3 = \text{pebbles}$, $w_4 = \text{rocks}$) through degrees of membership $\mu_{w_i}(x_k)$, with $0 \leq \mu_{w_i}(\cdot) \leq 1$. We assume independence between geometrical features F_{kj} , ($0 < j \leq 4$). Let $\mu_{w_i}(F_{kj})$ be the grades for each statistical parameter, which are issued from the membership function. Qualitatively, the membership function $\mu_{w_i}(F_{kj})$ expresses the strength of the belief that the detected cast shadow computed on sub-window k , with shape parameter F_{kj} , corresponds to the characteristic cast shadow shape of the class w_i . If $\mu_{w_i}(F_{kj}) = 1$, there is an absolute confidence that the detected cast shadows belong to the class w_i , whereas if $\mu_{w_i}(F_{kj}) = 0$, there is a null confidence. In our application, we model our *a priori* knowledge about the cast shadow shapes for each sea-bottom type by the following four assumptions:

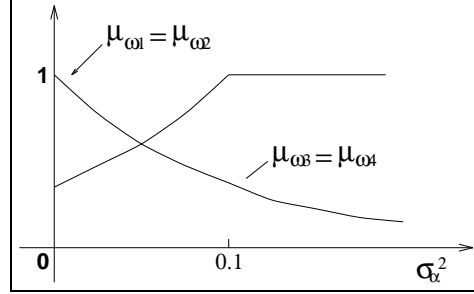


Figure 2: Plot of the membership functions for the parameter σ_α^2 .

1.) In case of ridge (label w_1) or dune (label w_2), cast shadow shapes have a common orientation, contrary to the ones created by the pebbles (label w_3) or rocks (label w_4). Therefore, we define empirically for parameter σ_α^2 the following membership functions:

$$\begin{aligned} \mu_{w_1}(\sigma_\alpha^2) &= \mu_{w_2}(\sigma_\alpha^2) \\ &= \exp(-\lambda_1 \sigma_\alpha^2) \\ \mu_{w_3}(\sigma_\alpha^2) &= \mu_{w_4}(\sigma_\alpha^2) \\ &= \begin{cases} \exp[-\lambda_1(\lambda_2 - \sigma_\alpha^2)] & \text{if } \sigma_\alpha^2 < \lambda_2 \\ 1 & \text{otherwise} \end{cases} \end{aligned}$$

We choose $\lambda_1 = 10$, $\lambda_2 = 0.1$ in our application. Fig. 2 represents the plot of the membership functions for this parameter.

2.) In case of ridge (label w_1) or dune (label w_2), cast shadows present a stretched shapes contrary to the ones created by the pebbles (label w_3) or rocks (label w_4). Therefore, we define for ξ_{max} :

$$\begin{aligned} \mu_{w_1}(\xi_{max}) &= \begin{cases} \exp[-\lambda_4(\lambda_5 - \xi_{max})] & \text{if } \xi_{max} < \lambda_5 \\ 1 & \text{otherwise} \end{cases} \\ \mu_{w_2}(\xi_{max}) &= \begin{cases} \exp[-\lambda_4(\lambda_6 - \xi_{max})] & \text{if } \xi_{max} < \lambda_6 \\ 1 & \text{otherwise} \end{cases} \\ \mu_{w_3}(\xi_{max}) &= \mu_{w_4}(\xi_{max}) \\ &= \begin{cases} \exp[-\lambda_4(\xi_{max} - \lambda_5)] & \text{if } \xi_{max} > \lambda_5 \\ 1 & \text{otherwise} \end{cases} \end{aligned}$$

We choose $\lambda_4 = 1$, $\lambda_5 = 7$, $\lambda_6 = 5$ ($\lambda_5 > \lambda_6$ since ridge cast shadows are stretchier than dune cast shadows).

3.) In case of ridges (label w_1) or dune (label w_2), cast shadows have less compact shapes than the ones created by pebbles (label w_3) or rocks (label w_4) that we can express by the following membership

function for C_{moy} :

$$\begin{aligned}
\mu_{w_1}(C_{moy}) &= \mu_{w_2}(C_{moy}) \\
&= \exp(-\lambda_6 C_{moy}) \\
\mu_{w_3}(C_{moy}) &= \mu_{w_4}(C_{moy}) \\
&= \begin{cases} \exp[-\lambda_6(\lambda_7 - C_{moy})] & \text{if } C_{moy} < \lambda_7 \\ 1 & \text{otherwise} \end{cases}
\end{aligned}$$

$\lambda_6 = 5$, $\lambda_7 = 0.2$ in our experiments.

4.) *Rock (label w_4) shadows have a bigger size than the ones created by pebbles (label w_3):* therefore, we define for C_{moy} :

$$\begin{aligned}
\mu_{w_3}(N_{max}) &= \begin{cases} \exp(\lambda_8 - N_{max}) & \text{if } N_{max} > \lambda_8 \\ 1 & \text{otherwise} \end{cases} \\
\mu_{w_1}(N_{max}) &= \mu_{w_2}(N_{max}) = 1 \\
\mu_{w_4}(N_{max}) &= 1 - \mu_{w_3}(N_{max})
\end{aligned}$$

we take $\lambda_8 = 60$ in our application. As we have assumed independence between the different geometrical features, the degree of membership for each class $w_i, \mu_{w_i}(x_k)$ ($0 < i \leq 4$) is given by the minimum operator [16]:

$$\mu_{w_i}(x_k) = \min \left\{ \mu_{w_i}(F_{k1}), \dots, \mu_{w_i}(F_{k4}) \right\} \quad 0 < i \leq 4$$

and we assign the class w_j to the sub-window k , satisfying:

$$\hat{w}_j = \arg \max_{w_j \in \{w_1, \dots, w_4\}} \{ \mu_{w_j}(x_k) \}$$

One has to find a good compromise for the size of sub-windows involved in the computation of feature vector x_k . On one hand, a small sub-window size increases the accuracy of the segmentation. On the other hand, geometrical features computed on a too small sub-window does not allow to efficiently recognize large cast shadow shapes such as the ones created by large dunes of sand (see Fig. 6). To circumvent this difficulty, a multi-scale classification is achieved by simply increasing the size of the sub-window in which we compute feature vectors x_k , and by taking into account the fuzzy classification results obtained at different scales. The classification strategy followed in our application, then consists in detecting the presence of the *dune* class at higher scale, and in projecting the detected dune label at the finest classification by duplication (see Fig. 3).

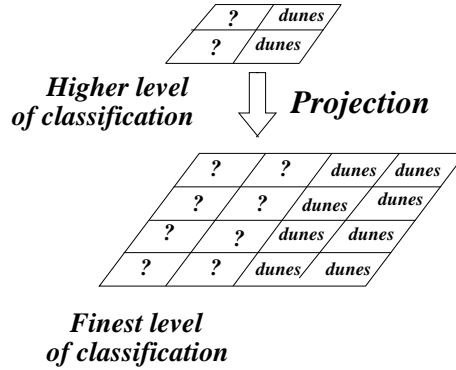


Figure 3: The multi-scale classification strategy.

4. SEGMENTATION STEP

In order to obtain an accurate segmentation-and-classification map, contextual information has to be taken into account. To this end, we resort to MRF models [15] which allows us both to take into account the fuzzy classification results previously obtained (on adjacent sub-windows) and also to express constraints on the desired solution such as homogeneity properties of the expected segmentation map. In this way, we consider a couple of random fields (X, W) , with $X = \{X_s, s \in S\}$, the field of observations (x_s the feature vector is considered as a realization of X_s), and $W = \{W_s, s \in S\}$ the label field, located on a lattice S of N sub-windows s . Each of the W_s takes its value in $\{w_0 = \text{sand}, w_1 = \text{ridges}, w_2 = \text{dunes}, w_3 = \text{pebbles}, w_4 = \text{rocks}\}$. The distribution of W , $P_W(w)$, is supposed to be stationary and Markovian. In this approach, the determination of segmentation map w is stated as a statistical contextual labeling problem, according to a global Bayesian formulation. We adopt the MAP criterion and we search for w such as:

$$\begin{aligned}\hat{w} &= \arg \max_w P_{W/X}(w/x) \\ &= \arg \max_w \{P_W(w) P_{X/W}(x/w)\}\end{aligned}$$

In accordance with the Hammersley and Clifford theorem [15], $P_W(w)$ is a Gibbs distribution ($P_W(w) \triangleq Z^{-1} \exp^{-U_2(w)}$ with $U_2(w)$, an energy function and Z a normalizing constant). Denoting $P_{X/W}(x/w) = \exp(-U_1(w, x))$, the above equation can be defined in terms of an energy function $U(w, x)$ to be minimized:

$$U(w, x) = U_1(w, x) + U_2(w)$$

where $U_1(w, x)$ is the “feature-driven” term that expresses the adequacy between observations and labels $\{w_0, w_1, w_2, w_3, w_4\}$, and $U_2(w)$ is the regularization energy term corresponding to the *a priori* model.

▷ Let $\mathcal{G} = \{\mathcal{G}_s, s \in S\}$ define a neighborhood system on S and \mathcal{C} the corresponding set of binary cliques. In order to favor homogeneous regions, we adopt a standard 8-connexity spatial neighborhood system for \mathcal{G} , and an isotropic Potts model that associates to binary clique $\langle s, t \rangle$ (see Fig. 4), the potential $V_{\langle s, t \rangle}(w) = \beta_{st}(1 - \delta(w_s, w_t))$ where β_{st} ($\beta_{st} \in \{\beta_1, \beta_2, \beta_3, \beta_4\}$) only depends on the orientation of the clique, and $\delta(\cdot)$ is the Kronecker delta function. $U_2(w)$ can then be written as:

$$U_2(w) = \sum_{\langle s, t \rangle} \beta_{st}(1 - \delta(w_s, w_t))$$

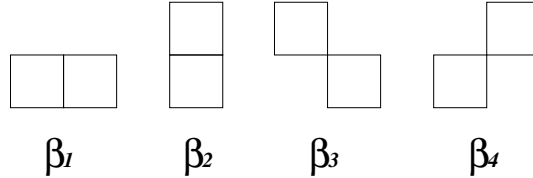


Figure 4: Two-site cliques and associated parameters.

▷ The interaction model between observations and hidden labels exploits the value obtained by the membership function $\mu_{w_i}(x_s)$ (see Section 3). $U_1(w, x)$ is defined as follows:

$$U_1(w, x) = - \sum_{s \in S} \gamma(w_s, x_s)$$

where $\gamma(\cdot)$ is a function that returns $\mu_{w_s}(x_s)$ if $w_s = \arg \max_{w_j} (\mu_{w_j}(x_s))$ ($0 \leq j \leq 4$) and 0 otherwise. Finally, the global energy function to be minimized is defined as follows:

$$U(w, x) = \underbrace{- \sum_{s \in S} \gamma(w_s, x_s)}_{U_1(w, x)} + \underbrace{\sum_{\langle s, t \rangle} \beta_{st}(1 - \delta(w_s, w_t))}_{U_2(w)}$$

U_1 expresses the adequacy between our *a priori* knowledge about the cast shadow shapes for each sea-bottom type and labels *via* the obtained result by the fuzzy pre-classification step. The second term U_2 encodes constraints on the desired solution such as homogeneity properties of the expected segmentation map. The optimal labeling we seek is the minimum of this energy function. We use the deterministic relaxation algorithm ICM [15] to minimize this function. For the initialization of this algorithm, we employ the classification map obtained by a blind fuzzy classification scheme.

5. EXPERIMENTAL RESULTS

To validate our sea-floor classification method, we have carried out experiments with images delivered by different sonar systems. For all the reported results, we consider a sub-window of 64×64 pixels size for the finest result classification (for cartography application, the considered accuracy level is sufficient and represents approximately a 6×6 meters area). For the multi-scale strategy classification (see Section 3), we use sub-windows of 128×128 and 256×256 pixels respectively. Potential parameters β_i are set to 0.2 ($0 < i \leq 4$).

Fig. 5, 6, 7, 8, 9 represent original sea-floor images and classification results obtained with our scheme with the following display convention superimposed on the original sonar image. An empty square for the class “sand”, and respectively a square with a small square inside it for the class “pebbles”, a bigger square for the class “rocks”, a straight line for the class “ridges” and two parallel lines for the class “dunes”. These sonar images are composed by one or several different sea-floor types and obtained results show good segmentation and classification results in all tested cases. We can also see the interest of our multi-scale classification strategy described in Section 3. It allows us to efficiently recognize large cast shadow shapes created sometimes by large dunes of sand. A right classification and segmentation map thanks to MRF regularization at full resolution is thus obtained. A look at Fig. 9.a and 9.b shows the improvement in classification by taking into account the spatial dependency between adjacent sub-windows, i.e., by using the Markovian *a priori* model described in Section 4. We can compare the results obtained with a simple feature extraction using a fuzzy classification scheme: less sub-windows are misclassified and the segmentation-and-classification map is more accurate. Remaining errors occur at the boundaries between different morphological elements, due to the possible mixture of classes of different natures that can occur (see Fig. 9.b). Nevertheless, experimental results demonstrate the accuracy and efficiency of such a contextual fuzzy segmentation and classification scheme.

6. CONCLUSION

We have presented an original approach to sea-floor classification combining MRF modeling and fuzzy logic. This pattern recognition scheme is based on the extraction and the identification of the cast shadow shapes of morphological elements lying on the sea-bed. The segmentation-and-classification issue is formulated in a Bayesian framework, and is stated as an equivalent energy minimization problem. This proposed scheme appears as an attractive alternative to classical textural feature-based extraction and neural classification approaches. This method has been validated on a number of real sonar images demonstrating the efficiency and robustness of this automatic scheme.

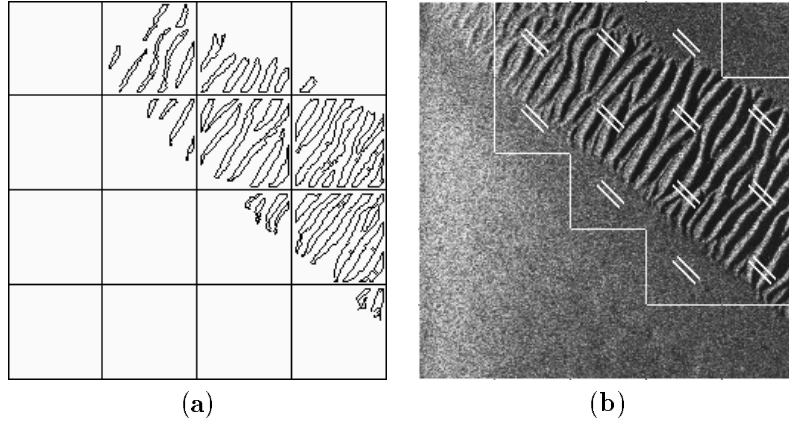


Figure 5: (a) Set of 1-labeled pixels of the binarized high pass filtered version of the segmented sonar image presented in (b). (b) Original sides-can sonar image of an area composed by sand (an empty square) and dune of sand (square with two parallel lines).



Figure 6: Original sidescan sonar image of an area composed by dunes (display convention: square with two parallel lines) and classification results obtained with our scheme. In this example, the adopted multi-scale classification strategy allows to efficiently recognize large cast shadow shapes created by dunes of sand and to obtain a right classification and segmentation map.

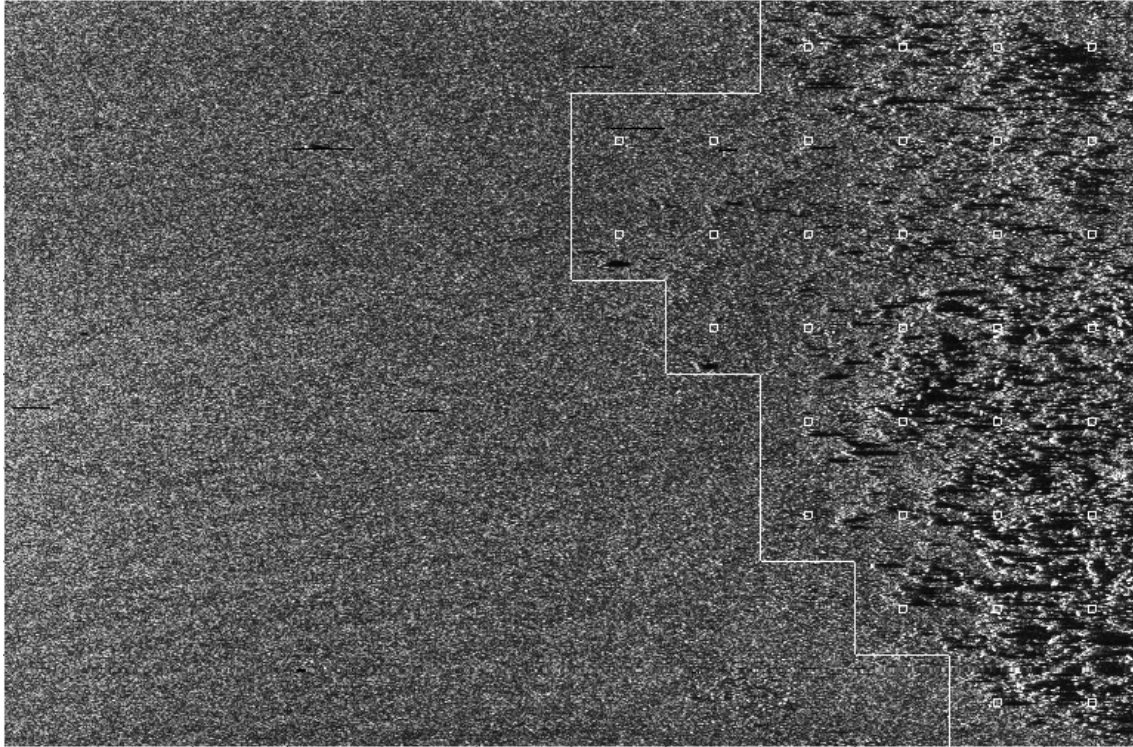


Figure 7: Original sidescan sonar image of an area composed of sand (display convention: empty square) and pebbles (display convention: square with a small square inside it). Segmentation and classification results showing right detection of these two classes.

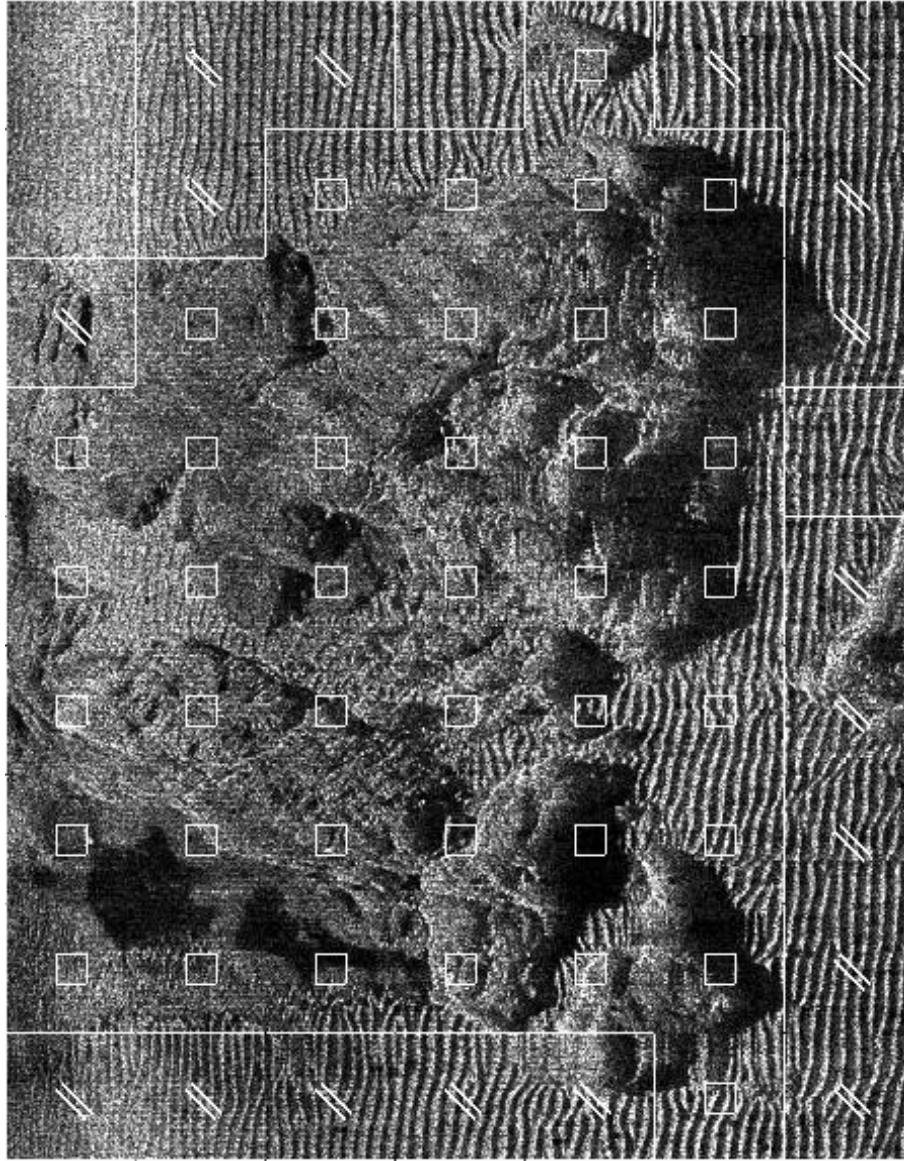


Figure 8: Original sidescan sonar image of an area composed by sand, rocks and ridges. segmentation and classification results showing right detection of these three classes.

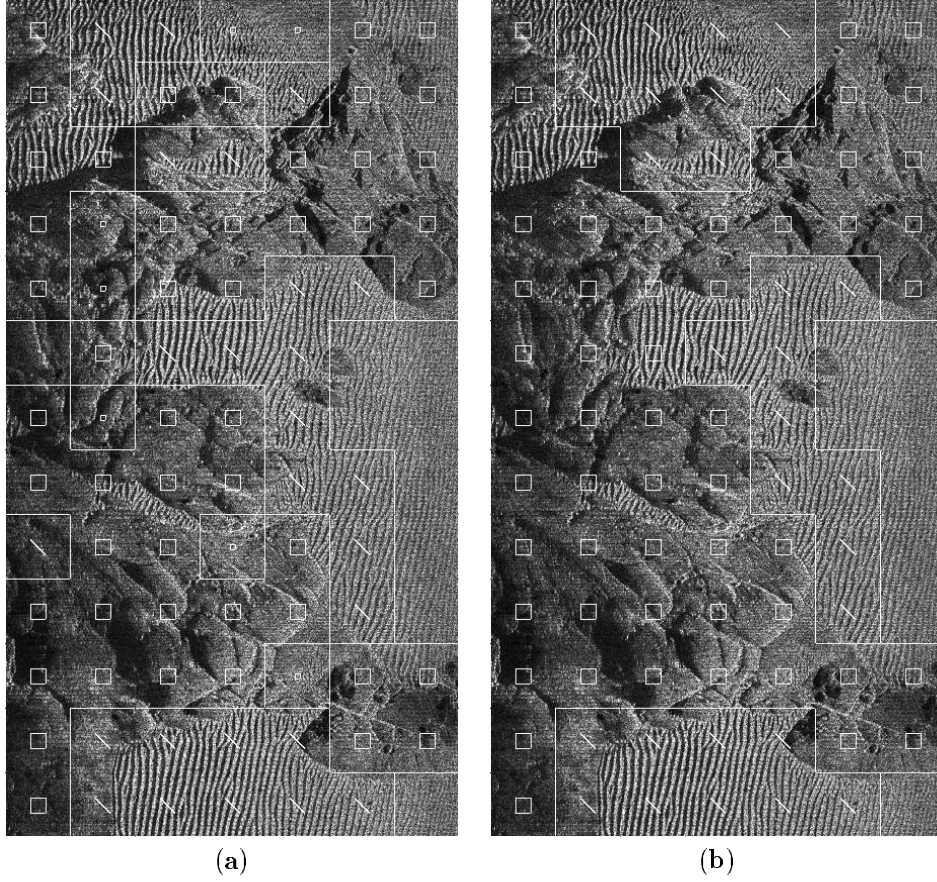


Figure 9: (a) Original sidescan sonar image composed by rocks and ridges and results obtained with a simple fuzzy classification scheme. (b) Classification results obtained with our scheme. In this example, we can see that contextual information allows to improve significantly the segmentation and classification results.

References

- [1] M. Mignotte, C. Collet, P. Pérez, and P. Bouthemy. Statistical model and genetic optimization: application to pattern detection in sonar images. In *Proc. IEEE International Conference on Acoustics, Speech, and Signal Processing*, volume V, pages 2541–2544, Seattle, May 1998.
- [2] B. Bourgeois and C. Walker. Sidescan sonar image interpretation with neural networks. In *Proc. OCEANS*, volume 3, pages 1687–1694, 1991.
- [3] S. Subramaniam, H. Barad, and A.B. Martinez. Seafloor characterization using texture. In *Proc. IEEE Southeastcon'93*, volume No 93CH3295-3, New Orleans, LA, USA, 4-7 April 1993.
- [4] B. Zerr, E. Maillard, and D. Gueriot. Sea-floor classification by neural hybrid system. In *Proc. OCEANS*, volume 2, pages 239–243, Brest, France, 13-16 Sept. 1994.
- [5] W.K Stewart, M. Jiang, and M. Marra. A neural network approach to classification of sidescan sonar imagery from a midocean ridge area. *IEEE Journal of Oceanic Engineering*, 19(2):214–224, Apr. 1994.
- [6] D.T. Cobra and H.A de Moraes. Classification of side-scan sonar images through parametric modeling. In *Proc. OCEANS*, volume 2, pages 461–464, Brest, France, 13-16 Sept. 1994.
- [7] H. Thomas, C. Collet, K. Yao, and G. Burel. Some improvements of a rotation invariant autoregressive method: Application to the neural classification of noisy sonar images. In *IXeme European Signal Processing Conference - EUSIPCO'98*, volume IV, pages 2001–2004, Rhodes Island, Greece, September 1998.
- [8] D. Vray, P. Delachartre, N. Andrieux, and G. Gimenez. Bottom classification using information in the spectral domain and time-frequency domain. In *Proc. OCEANS*, volume 2, pages 659–664, Brest, France, 13-16 Sept. 1994.
- [9] D.R. Carmichael, L.M. Linnet, S.J. Clarke, and B.R. Calder. Seabed classification through multifractal analysis of sidescan sonar imagery. *IEE Proc. Radar, Sonar Navig.*, 143(3):140–148, June 1996.
- [10] J. W. Goodman. Some fundamental properties of speckle. *Journal of Optical Society of America*, 66(11):1145–1150, Nov. 1976.
- [11] F. Schmitt, M. Mignotte, C. Collet, and P. Thourel. Estimation of noise parameters on sonar images. In *Signal and Image Processing*, volume SPIE 2823, pages 1–12, Denver, Colorado, USA, Aug. 1996.
- [12] M. Mignotte, C. Collet, P. Pérez, and P. Bouthemy. Unsupervised hierarchical Markovian segmentation of sonar images. In *Proc. 4th IEEE International Conference on Image Processing*, Santa Barbara, CA, USA, Oct. 1997.
- [13] D. Alexandrou and D. Pantzartzis. Seafloor classification with neural networks. In *Proc. OCEANS*, volume I, pages 18–23, 1990.
- [14] D. Alexandrou and D. Pantzartzis. A methodology for acoustic seafloor classification. *IEEE Journal of Oceanic Engineering*, 18(2):81–86, Apr. 1993.
- [15] J. Besag. On the statistical analysis of dirty pictures. *Journal of the Royal Statistical Society*, B-48:259–302, 1986.
- [16] L.A. Zadeh. *Fuzzy sets as a basis for a theory of possibility. Fuzzy Sets and Systems 1*. Addison-Wesley, 1978.